IEEE Robotics and Automation Letters (RAL) paper presented at the
2020 IEEE/RSJ International Conference on Intelligent Robots and Systems (IROS)
October 25-29, 2020, Las Vegas, NV, USA (Virtual)

A Control Scheme for Smooth Transition in Physical Human-Robot-Environment between two Modes: Augmentation and Autonomous

Hsieh-Yu Li[1], Liangjing Yang[2], *Member, IEEE*, and U-Xuan Tan[1], *Member, IEEE*

***Abstract*— There has been an increasing demand for physical human-robot collaboration during the design prototyping phase. For example, users would like to maneuver the end-effector compliantly in free space followed by supplying a contact force to obtain a firm adhesive connection. The technical challenges is the design of the controller, especially during the switching from human-robot interaction (human guides robot) to robot-environment interaction for the robot to continuously maintain the contact force even after the human lets go. Traditional controllers often result in unstable interaction during the switches of the controllers. Therefore, this paper proposes a control scheme that unifies impedance and admittance in the outer loop, and unifies the adaptive position and velocity control in the inner loop to address this issue. The cooperation of the cobot is divided into two modes, namely, an augmentation mode where the human force is the desired input to guide the motion of the cobot, and an autonomous mode where predefined position and force commands are used (e.g., to maintain a desired holding force). With the proposed control scheme, the physical interaction between the robot, human and environment can be smoothly and stably transited from augmentation mode to autonomous mode. Experiments are then conducted to validate the proposed approach.**

I. INTRODUCTION

Collaborative robots (cobot) have gained increasing importance as it can work with human closely. Cobots can be used in different ways according to the tasks. One type of cobot, or augmentation mode, is where human operator is able to direct the motion of the cobot [1], [2], exerting his/her forces on the force/torque (F/T) sensor mounted at the end-effector of the robot. The main feature for this type of cobot is that no pre-defined position or force commands are required. Hence, the human can guide the cobot to any position with his/her judgement while the cobot augments the human force to execute the tasks. To achieve this physical human-robot interaction (pHRI), common proposed controllers include force control [3], [4] or admittance control [5], [6], [7] which transfers the human force into the robot velocity.

There has been increasing need for this cobot with an augmentation mode to extend pHRI to physical human-robot-environment interaction (pHREI) [8]-[11] to widen the range of applications. The concept of this topic is that external forces on the end-effector (minus human force) are considered environmental forces. When a human guides the robot end-effector from free space to contact an environment, the interaction might not be stable as the F/T sensor includes both human and environmental forces. As shown in Fig. 1 (A), the researchers [9], [10] propose two F/T sensors to address this issue. By separating these two external forces, a stable interaction is achieved. Potential applications include human-robot augmentation [9] and medical robots [10], [11].

However, such a controller for an augmentation mode cobot is not able to handle situations which require the robot to autonomously interact with the environment after the human guides the robot to the desired location. This is because the desired commands are human forces, and the motion output becomes zero after the human releases the cobot. To autonomously interact with the target, a controller that has predefined position or force commands to interact with the human or environment is highly desired. We define that such a cobot is operated under an autonomous mode. The cobot in this mode is typically used to handle physical robot-environment interaction (pREI) [14], [15], [16], [23].

Although considerable research has been devoted to cobots in both augmentation and autonomous mode, the two modes have been predominantly studied in isolation. This limits the flexibility and potential applications. For example, a medical cobot in the augmentation mode can be a great assistance for the surgeon to improve the accuracy [4]. Nonetheless, the cobot in this augmentation mode requires the manual guidance from the surgeon or nursing staff at all times. The lack of the autonomy causes the inefficacy and becomes a burden without human intervention. Anther example of such situation is the smart phone assembly during new product introduction (NPI). During NPI, automation is expensive to be implemented in the design phase as the parts and components are not yet fixed, and multiple manual assembly steps are required. When the bodies of the phone are combined, a waterproof adhesive strip tape is used to ensure the phone is connected well. To achieve a good adhesive connection, the engineer needs to press the phone with a sufficient force for over a period of time. This process is tiring as there may be hundreds of phones that need to be assembled. Therefore, it appears that the source of the gap stems from the needs to incorporate a scheme to transfer the controllers from the augmentation to the autonomous mode.

The situation using two modes is shown as Fig. 1. The human can guide the robot to press the target on the environment as shown in Fig. 1(A) using a cobot with an

[1]H.-Y. Li and U.-X. Tan are with Pillar of Engineering Product Development, Singapore University of Technology and Design, Singapore hsiehyu_li@sutd.edu.sg, uxuan_tan@sutd.edu.sg

[2]L. Yang is with Zhejiang University/University of Illinois at Urbana-Champaign Institute, China liangjingyang@intl.zju.edu.cn

augmentation mode. After the interactive force in pHREI is stabilized, the human presses a switch and releases the robot, as shown in Fig. 1(B). The controller switches into another control scheme using autonomous mode for pREI and the robot will press the target by maintaining the contacting force, as illustrated in Fig. 1(C). For pREI, the impedance control [12]-[14], or hybrid position/force control [18] is typically used for an cobot with autonomous mode to maintain the position while keeping the contacting force with the environment.

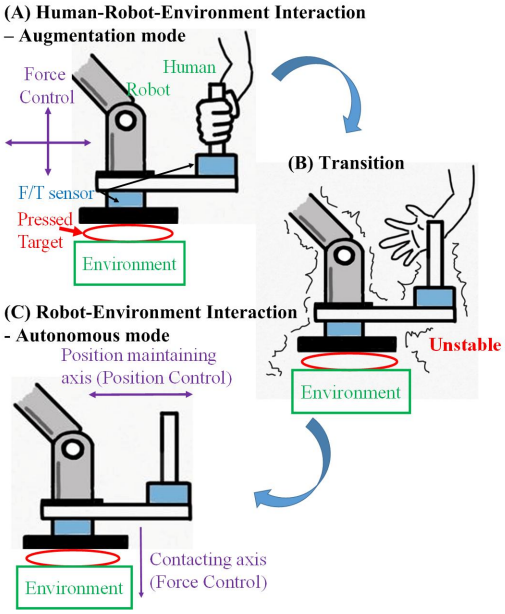

Fig. 1. Research topic and problem. This paper focuses on the issue of the unstable transition in (B) from pHREI in (A) to pREI in (C). The difficulty lies on designing a proper control scheme to switch from the augmentation mode to the autonomous mode during pHREI in (B).

There are three main technical challenges for this transition during pHREI. Firstly, to maintain the same position robustly, the controller needs to switch from force control to position control, like the position maintaining axis in Fig. 1(C). During this transition, it causes risk of instability as the control structures change, as shown in Fig. 1(B). This is especially true for the case where a rapid response is needed. Secondly, the contacting axis (Fig. 1(C)) also requires the transition between force control where the desired force is from human to another force control where the desired force is a constant to maintain the interaction with the environment after the human releases the robot. There is a change of the net force from human, robot and environment to only robot and environment interaction, creating the challenge to achieve smooth transition without force overshoot while maintaining a stable interaction. The last issue is the controller parameters transition for different interaction. The objectives of robot interaction with human and environment are different [10], [19], such as the collaboration should be compliant to human intended motion while the interaction should be stable to a rigid environment. It makes the parameter transitions for different interaction difficult.

The bottleneck for smooth transition between two modes during the robot interaction with human and environment lies in a proper control scheme. Therefore, in this paper, we propose a control scheme that unifies impedance/admittance and unifies adaptive position/velocity control to address the issue. This unified control scheme can switch between the two modes where human force is the desired input or where the robot autonomously interacts with the environment.

There are two main contributions. Firstly, unlike the existing research for the controller design only focusing on pHRI [2], [5], [6] or pREI [12]-[17], we target the topic of pHREI. In particular, in this paper, we aim to address a different issue where the unstable transition occurs when the physical interaction is transferred between human, robot and environment. A control scheme is proposed to ensure the robot interaction can be smoothly and seamlessly transferred to any objects. Secondly, this paper is different from the existing research which discuss the controller transition for a cobot with a single mode. The focus on the existing research of the control transition is mostly about the autonomous mode. The physical robot interaction typically transfers from no environment to in contact with an environment [15], [16], or from interaction with a human to no interaction with any object [20]. The transition happens upon either a sharp human/environment force increases or the trajectory deviates off the predefined desired path. On the contrary, the control transition for a cobot with the augmentation mode has seldom been investigated. In addition, the proposed approach in this paper leverages the control transition between two modes, which aims to overcome the limitation of existing method where the human could not provide the intelligence to decide the transition moment based on the situations.

II. Preliminary

A. Robot Dynamics

The dynamics of a robotic manipulator [20], [21] are described by

$$M(q)\ddot{q}+C(q,\dot{q})\dot{q}+g(q)=\tau+J^T(q)F_{ext} \tag{1}$$

where $q,\dot{q},\ddot{q}\in R^n$ are the robot position, velocity and acceleration in joint space, n is degree-of-freedom (DOF), and $M(q),C(q,\dot{q})$, g are the inertia matrix, Coriolis/Centripetal vector and gravity vector. τ is the joint control torques and F_{ext} is the external forces exerting on the robot. $J(q)$ is the robot Jacobian. The relation between control torque and force is $\tau=J^TF$ where F is the control force in Cartesian space. Additionally, assume $x,\dot{x},\ddot{x}$ are the robot position, velocity and acceleration in Cartesian space where $x=h(q)$ and $h(\cdot)$ is the forward kinematics. Hence, $\dot{x}=J(q)\dot{q},\ddot{x}=J(q)\ddot{q}+\dot{J}(q)\dot{q}$.

B. External Force

In this pHREI research, the external force is composed of the human force, F_h, and environmental force, F_{en}. The free body diagram (FBD) is as shown in Fig. 2 (A) and

$$F_{ext}=F_h+F_{en}. \tag{2}$$

The human force can be detected in the F/T sensor. To save the cost of the second F/T sensor, in this paper, we use an force estimator to get F_{en}. More specifically, a well-known force estimator [22], [26] based on generalized momentum is employed for F_{ext}. Define a residual vector r as

$$r \equiv K_r \left[p - \int_0^t \left(\tau + C^T(q,\dot{q})\dot{q} - g(q) \right) d\varsigma \right] \tag{3}$$

where K_r is a positive gain (diagonal) and $p = M(q)\dot{q}$. The estimated external force is $\hat{F}_{ext} = J^T(q)r$ and assume $\hat{F}_{ext} \equiv F_{ext}$. Therefore, the environmental force can be estimates as

$$\hat{F}_{en} = \hat{F}_{ext} - F_h. \tag{4}$$

C. Impedance/Admittance Control in pHRI/pREI

The common practice for impedance control in pREI with autonomous mode [12], [14], [23] is to ensure the position error is compliant or rigid according to the desired contact force or environmental force. The target impedance in the outer loop is designed as

$$M_d\ddot{e} + B_d\dot{e} + K_d e = -F_d - F_{en} \tag{5}$$

where the position error is $e = x_d - x_m$, and M_d, B_d, K_d are the desired impedance inertia, damping and stiffness. F_d is the desired contacting force, x_d is the desired position and x_m is the generated virtual position input for position control in the inner loop. If there are no desired or environmental force ($F_d, F_{en} = 0$), the goal is to attain $x \to x_m \to x_d$ like position control. On the contrary, this controller behaves like force tracking [14], [23] when $F_d, F_{en} \neq 0$ as x_m changes according to F_d, F_{en}.

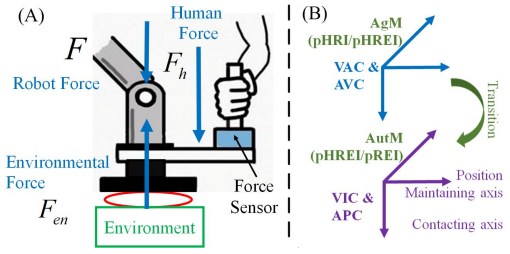

Fig. 2. (A) Free body diagram of human-robot-environment interaction (1 DOF, contacting axis). (B) The controller transition from AgM to AutM.

On the other hand, the common admittance control scheme for pHRI with the augmentation mode [1], [2], [5], [6] is to take human forces as input and engender velocity output. The target admittance in the outer loop is designed as

$$M_d\ddot{x}_m + B_d\dot{x}_m = F_h \tag{6}$$

where $\dot{x}_m, \ddot{x}_m$ are the generated virtual velocity and acceleration input to the velocity control in the inner loop. The goal of this controller is to ensure the input $\dot{x}_m$ which is generated by admittance attain perfect tracking in velocity loop, i.e., $\dot{x} \to \dot{x}_m$. Both impedance (5) and admittance (6) are used in the proposed control scheme and will be discussed later.

D. Notations

In this paper, we consider two modes in a cobot for the above-mentioned interaction, namely, augmentation mode (AgM) and autonomous mode (AutM). Particularly, AgM is where the human operational force is the desired force of the cobot and human can direct the motion of the cobot. The interaction in AgM includes pHRI and pHREI. On the contrary, AutM is that the cobot autonomously interacts with the environment, by position or force control, and human force is considered as disturbance. The interaction in AutM includes pHREI and pREI.

III. Proposed Method

As illustrated in Fig. 2 (B), a variable admittance controller (VAC) at outer loop and adaptive velocity control (AVC) in the loop is employed in AgM. It allows the human to direct the motion of the robot and the controller performs like "force control". On the other hand, in AutM, we use variable impedance control (VIC) with adaptive position control (APC) to maintain the position accurately in the position maintaining axis while keeping the contacting force in the contacting axis. With these two controllers, the unified control scheme is proposed as shown in Fig. 3 which consists of (A) outer loop for interaction control, and (B) inner loop for motion control and compensation of unknown dynamics.

A. Outer Loop: Unified Variable Admittance/Impedance Control

The unified target admittance and impedance is combined from (5) and (6) as

$$M_d(\Phi\ddot{x}_d - \ddot{x}_m) + \hat{B}_d(\Phi\dot{x}_d - \dot{x}_m) + \Phi K_d(x_d - x_m) = -F_{ta} \tag{7}$$

where $M_d \in R^{nxn}, K_d \in R^{nxn}$ are the desired constant impedance/admittance inertia and stiffness respectively, which are positive and diagonal. $\hat{B}_d \in R^{nxn}$ is the desired variable damping which is also positive and diagonal. The update law for $\hat{B}_d$ will be discussed later.

Firstly, Φ is the transition factor defined as

$$\Phi = \begin{cases} 0, & \text{AgM} \\ 0-1, & \text{Transition} \\ 1, & \text{AutM} \end{cases} \tag{8}$$

During the transition from AgM to AutM, Φ increases from 0 to 1 within a transition time t_t with gradient $1/t_t$ and vice versa, reduces from 1 in AutM to 0 in AgM with slope $-1/t_t$. The moment to change to another control scheme is decided by human using a switch. F_{ta} is the modified target force

$$F_{ta} = (1-\Phi)K_h F_h + \Phi F_d + \hat{F}_{en} \tag{9}$$

where K_h is a constant proportional gain for the human force and F_d is the desired constant force for the contacting axis. With this design, during AgM ($\Phi = 0$), eq (7) becomes VAC where the controller takes force (F_h or $\hat{F}_{en}$) as input and engenders velocity commands $\dot{x}_m$ to the velocity controller. The target admittance becomes $M_d\ddot{x}_m + \hat{B}_d\dot{x}_m = K_h F_h + \hat{F}_{en}$. When there is no environmental force ($\hat{F}_{en} = 0$), it behaves

like transitional pHRI [1], [6] as the desired force input is only the human augmented force $K_h F_h$. When there exists an environment force ($\hat{F}_{en} \neq 0$), it becomes the controller for pHREI to stabilize the interaction [10]. On the other hand, during AutM ($\Phi = 1$), eq (7) becomes target impedance (5) with variable damping where the target force $F_{ta} = F_d + \hat{F}_{en}$ are in response of desired motion x_d. For the position maintaining axis, we design $F_d = 0$. Therefore, it can behave like position control to reject disturbance $\hat{F}_{en}$. For the contacting axis, we set F_d to be the augmented human force $K_h F_h$ before the controller switches from AgM to AutM. Hence, it behaves like force tracking impedance control [14], [23].

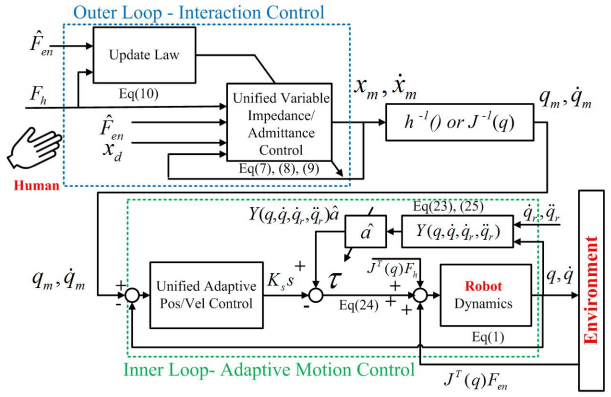

Fig. 3. The proposed control scheme.

Secondly, the update law for damping is proposed as

$$\hat{B}_d = B_0\big[1 - \underbrace{\alpha_h |F_h|}_{\text{Human Interaction}} + \underbrace{\alpha_{en}|\hat{F}_{en}|}_{\text{Environment Interaction}} \underbrace{-\Phi\alpha_t|F_d + \hat{F}_{en}|)}_{\text{Transition}}\big] \tag{10}$$

where B_0 is the initial value of damping, $\alpha_h, \alpha_{en}, \alpha_t$ are the gains to update the human force, environmental force and the force error $F_d + \hat{F}_{en}$, which are all positive definite and diagonal. The first term updating the human interaction is like traditional VAC in pHRI, i.e. increasing the admittance when the human intended acceleration is higher and decreasing the admittance when it is lower (more about VAC for pHRI can be found in [2], [6]). The second term updating the environmental interaction is that the admittance should reduce when the environmental force is larger to decrease the sensitivity of force exchange, and vice versa (more about VAC for environmental interaction can be found in [10]). The last term is our proposed update law for transition. When human releases the robot, the net force of the interaction changes into only the robot and environment which leads to the decrease of the environmental force. This also increases the force error $F_d + \hat{F}_{en}$. The proposed term increases the admittance when the force error increases. This results in faster compensation for force error and a smoother transition.

Thirdly, the motion commands generated by the target variable impedance/admittance (7) can be derived as

$$\dot{x}_m(t) = \int_0^t \Big\{ \Phi\ddot{x}_d(\varsigma) + M_d^{-1}\big[\hat{B}_d(\varsigma)\big(\Phi\dot{x}_d(\varsigma) - \dot{x}_m(\varsigma)\big) + \Phi K_d\big(x_d(\varsigma) - x_m(\varsigma)\big) + F_{ta}(\varsigma)\big]\Big\} d\varsigma \tag{11}$$

$$x_m(t) = \int_0^t \dot{x}_m(\varsigma) d\varsigma. \tag{12}$$

Lastly, since the goal for AutM is to maintain the position and maintain the contacting force, we set the velocity and acceleration to be 0, i.e., $\dot{x}_d, \ddot{x}_d = 0$. The desired position, x_d is set to be equal to x during AgM. During AutM, x_d is set to be a constant value and is equal to the last position of robot before we switch from AgM to AutM. In other words,

$$x_d(t) = \begin{cases} x(t), & \text{AgM} \\ x_d(t_s), & \text{Transition or AutM} \end{cases} \tag{13}$$

where t_s is the latest switch time.

Assumption 1: Define $\tilde{r} = \tau_{ext} - r$ as the estimated external torque error. In addition, assume the external torque τ_{ext} is slowly time-varying [29], [30].

Based on assumption 1, the force estimation error achieves asymptotic stability [30], [35]. In other words, $\hat{F}_{en} \to F_{en}$. This can be proved by a Lyapunov function $V_r = \frac{1}{2}\tilde{r}^T K_r^{-1}\tilde{r}$ and $\dot{V}_r = -\tilde{r}^T\tilde{r}$. More details can be found in [30], [35].

Theorem 1: The proposed unified impedance/admittance (7) with the update law (10) ensures a passive mapping between the proposed target force (9) and the generated motion commands (11) as long as the condition of the stationary motion, i.e., $\dot{x}_m = 0$, is met during the transition.

Proof: Since $\dot{x}_d, \ddot{x}_d = 0$, the target impedance/admittance (7) becomes

$$M_d\ddot{x}_m + \hat{B}_d\dot{x}_m - \Phi K_d e = F_{ta} \tag{14}$$

For AutM and transition ($\Phi \neq 1$), we choose a storage function

$$V_s = \frac{1}{2}\dot{x}_m^T M_d \dot{x}_m + \frac{1}{2}e^T K_d e. \tag{15}$$

Since $\dot{e} = -\dot{x}_m$, the derivative of V_s is

$$\begin{aligned} \dot{V}_s &= \dot{x}_m^T M_d \ddot{x}_m + \dot{e}^T K_d e \\ &= \dot{x}_m^T\big(-\hat{B}_d\dot{x}_m + \Phi K_d e + F_{ta}\big) + \dot{e}^T K_d e \\ &= \dot{x}_m^T\big(-\hat{B}_d\dot{x}_m + \Phi K_d e + F_{ta}\big) - \dot{x}_m^T K_d e \\ &= -\dot{x}_m^T\hat{B}_d\dot{x}_m + \dot{x}_m^T F_{ta} - \dot{x}_m^T(1-\Phi)K_d e. \end{aligned} \tag{16}$$

Rearranging the terms and taking integral

$$\begin{aligned} &\int_0^t \dot{x}_m^T(\varsigma)F_{ta}(\varsigma)d\varsigma = V_s(t) - V_s(0) \\ &+ \int_0^t \big[\dot{x}_m^T(\varsigma)\hat{B}_d\dot{x}_m(\varsigma) + \dot{x}_m^T(\varsigma)(1-\Phi(\varsigma))K_d e(\varsigma)\big]d\varsigma \\ &= V_s(t) - V_s(0) + \int_0^t W(\varsigma)d\varsigma \end{aligned} \tag{17}$$

where $\int_0^t W(\varsigma)d\varsigma$ is considered as the dissipated energy [5], [10], [21]. To ensure passive mapping between input F_{ta} and output $\dot{x}_m$, the dissipated energy must be greater than 0 [10],

[24], [25]. When $\Phi = 1$, $\int_0^t W(\varsigma)d\varsigma \geq 0$ since $\hat{B}$ is positive definite. On the other hand, during the transition $0 < \Phi < 1$, if $\dot{x}_m = 0$, we can also obtain $\int_0^t W(\varsigma)d\varsigma = 0$. In other words, the required condition for transition moment is when the interaction is stable and robot is stationary, $\dot{x}_m = 0$. From [9], [10], when $\Phi = 1$, and when the human, the robot and the environment are in contact, if the controlled system is passive, the human augmented force will eventually be equal to environmental force, i.e. $K_h F_h = -F_{en}$. From assumption 1, $F_{en} = \hat{F}_{en}$. When $K_h F_h = -\hat{F}_{en}$ and $\Phi = 1$, it implies $F_{ta} = 0$, leading to $\dot{x}_m = 0$ and means the robot motion is stationary.

Similar to above, in AgM ($\Phi = 0$), we modify V_s as

$$V_s = \frac{1}{2}\dot{x}_m^T M_d \dot{x}_m. \tag{18}$$

This form of storage function is the traditional VAC for pHRI [1], [10]. The passivity is guaranteed as $\int_0^t \dot{x}_m^T(\varsigma)F_{ta}(\varsigma)d\varsigma = V_s(t) - V_s(0) + \int_0^t \dot{x}_m^T(\varsigma)\hat{B}_d\dot{x}_m(\varsigma)d\varsigma \geq 0$ if $\hat{B}_d > 0$. ■

B. Inner Loop: Unified Adaptive Position/Velocity Control

The goals of the inner loop are: (i) to achieve idealized trajectory tracking (position or velocity), i.e., $x \to x_m, \dot{x} \to \dot{x}_m$; (ii) to compensate the uncertainty of robot dynamics; and (iii) to switch between position and velocity. Hence, the unified sliding vector is proposed as

$$s = \dot{\tilde{q}} + \Phi\Lambda_{sp}\tilde{q} + (1-\Phi)\Lambda_{sv}\int_0^t \dot{\tilde{q}}(\varsigma)d\varsigma \tag{19}$$

where $\tilde{q} = q - q_m$ is the trajectory error, $\dot{q} = J^{-1}(q)\dot{x}$ and $\dot{q}_m = J^{-1}(q)\dot{x}_m$. $\Lambda_{sp}, \Lambda_{sv}$ are the positive gain for position control and velocity control respectively. If $\Phi = 0$ (AgM), the first and third term are integral adaptive sliding signal [19], [27] for the adaptive velocity control. While $\Phi = 1$ (AutM), the first and second term of (19) becomes adaptive position control [20], [28]. Defining a reference vector $\dot{q}_r$ as

$$\dot{q}_r = \dot{q}_m - \Phi\Lambda_{sp}\dot{\tilde{q}} - (1-\Phi)\Lambda_{sv}\int_0^t \dot{\tilde{q}}(\varsigma)d\varsigma. \tag{20}$$

With (20), the sliding vector can be modified into traditional way [20], [21], [28] as

$$s = \dot{q} - \dot{q}_r, \dot{s} = \ddot{q} - \ddot{q}_r. \tag{21}$$

The beauty of this proposed controller is that, no matter which mode the robot is operated in, equation (21) is always true. Therefore, using the sliding vector (21), the open-loop model (1) can be represented in a traditional closed-loop non-linear time-varying form with the regressor [28],

$$M(q)\dot{s} + C(q,\dot{q})s + Y(q,\dot{q},\dot{q}_r,\ddot{q}_r)a = \tau + \tau_{ext} \tag{22}$$

where $\tau_{ext} = \tau_h + \tau_{en}$ and $\tau_{en} = J^T F_{en}, \tau_h = J^T F_h$. $Y(q,\dot{q},\dot{q}_r,\ddot{q}_r)a = M(q)\ddot{q}_r + C(q,\dot{q})\dot{q}_r + g(q)$ with regard to $\Phi = 0$ or 1. $a \in R^n$ is unknown dynamic parameter and $Y(q,\dot{q},\dot{q}_r,\ddot{q}_r) \in R^{nxn}$ is a known dynamic regressor matrix. In the presence of uncertainty for robot dynamics with the unknown dynamic parameters $\hat{a}$, we can obtain

$$Y(q,\dot{q},\dot{q}_r,\ddot{q}_r)\hat{a} = \hat{M}(q)\ddot{q}_r + \hat{C}(q,\dot{q})\dot{q}_r + \hat{g}(q) \tag{23}$$

where $\hat{a}$ denotes the estimation of a, and $\hat{M}(q), \hat{C}(q,\dot{q}), \hat{g}(q)$ represent the estimated models for $M(q), C(q,\dot{q}), g(q)$, respectively [20]. Therefore, the proposed control law for the unified adaptive position and velocity controller can also be proposed in a traditional form [20], [28]

$$\tau = Y(q,\dot{q},\dot{q}_r,\ddot{q}_r)\hat{a} - K_s s \tag{24}$$

where K_s is a sliding gain (positive definite matrix) for s. The update law for the unknown parameters is

$$\dot{\hat{a}} = -\Gamma Y^T(q,\dot{q},\dot{q}_r,\ddot{q}_r)s \tag{25}$$

where Γ is the adaptive gain (positive definite matrix). Substituting (24) into (23), the closed-loop dynamics is

$$M(q)\dot{s} + C(q,\dot{q})s + K_s s + Y(q,\dot{q},\dot{q}_r,\ddot{q}_r)\tilde{a} = \tau_{ext} \tag{26}$$

where $\tilde{a} = a - \hat{a}$ denotes the estimated unknown parameter error.

Theorem 2: The closed-loop dynamic (26) guarantees: (i) when there exists external torque, it shows a passive mapping between external torque and sliding vector; and (ii) when there is no external torque, the tracking error $\tilde{q}, \dot{\tilde{q}}$ converges and estimated external torque error $\tilde{r}$ converges if the robot is not in the singularity pose.

Proof: Lyapunov candidate is chosen as

$$V = \frac{1}{2}s^T M(q)s + \frac{1}{2}\tilde{a}^T\Gamma^{-1}\tilde{a} + \frac{1}{2}\tilde{r}^T K_r^{-1}\tilde{r}. \tag{27}$$

Taking the derivative of V, substituting the control law (24), and using the update law (25) and the property of $s^T(\dot{M}(q) - 2C(q,\dot{q}))s = 0$ [13], [20], [23], we have

$$\begin{aligned}\dot{V} =& s^T M(q)\dot{s} + \frac{1}{2}s^T\dot{M}(q)s - \dot{\hat{a}}^T\Gamma^{-1}\tilde{a} + \dot{\tilde{r}}^T\tilde{r} \\ =& s^T\left[-C(q,\dot{q})s - K_s s - Y(q,\dot{q},\dot{q}_r,\ddot{q}_r)\tilde{a} + \tau_{ext}\right] \\ &+ \frac{1}{2}s^T\dot{M}(q)s - \dot{\hat{a}}^T\Gamma^{-1}\tilde{a} - \tilde{r}^T\tilde{r} \\ =& -s^T K_s s - \tilde{r}^T\tilde{r} + s^T\tau_{ext}.\end{aligned} \tag{28}$$

Taking integral for both side and rearranging the terms,

$$\begin{aligned}&\int_0^t s^T(\varsigma)\tau_{ext}(\varsigma)d\varsigma = V(t) - V(0) \\ &+ \int_0^t \left[s^T(\varsigma)K_s s(\varsigma) + \tilde{r}^T(\varsigma)\tilde{r}(\varsigma)\right]d\varsigma.\end{aligned} \tag{29}$$

Since K_s is positive definite, it shows the passive mapping between s and external torque τ_{ext}. If $\tau_{ext} = 0$, we can obtain $\dot{V} = -s^T K_s s - \tilde{r}^T\tilde{r} \leq 0$. Because $V > 0$ and $\dot{V} \leq 0$, V is bounded, which implies $s, \tilde{r}$ are also bounded and therefore $\dot{V}$ is bounded. According to Barbalat's Lemma [25], [20], [28], $\dot{V} \to 0$ as $t \to \infty$. $\dot{V} \to 0$ implies $s \to 0$ and $\tilde{r} \to 0$ which also implies that both $\tilde{q}$ and $\dot{\tilde{q}}$ tend to 0 as t tends to infinity. One thing to take note is that the robot must not be in singularity position for this method such that J^{-1} is not infinite and $q_m, \dot{q}_m$ exist. Hence, $\tilde{q}, \dot{\tilde{q}} \to 0$ implies $\tilde{x}, \dot{\tilde{x}} \to 0$, and $\tilde{r} \to 0$ implies $r \to \tau_{ext}$ so as $\hat{F}_{en} \to F_{en}$. ■

IV. Experiments

A. Experimental Setup

As shown in Fig. 4, we design a 3-DOF robot with a Cartesian structure to validate the idea. This robotic system is implemented in a RT (Real-Time) controller, CompactRIO (cRIO-9035; National Instrument Inc., USA). An ATI Nano-25 F/T sensor (ATI Industrial Automation Inc., USA) is mounted in the end-effector to measure the human forces. The environment is setup as a flat wooden platform. The human operator grasps a operational holder that is mounted on the F/T sensor, and contacts the environment with the end-effector that is separated from the holder. A physical mechanical contact switch is used to change in between AgM and AutM.

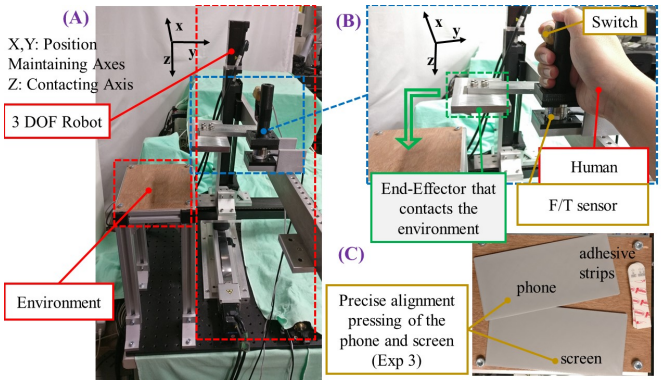

Fig. 4. The experimental setup.

The proposed controller is implemented in XYZ axes with the parameters of $M_0 = \text{diag}\{45,10,5\}$kg, $B_0 = \text{diag}\{180,300,200\}$Ns/m, $K_0 = \text{diag}\{50,40,10\}$N/m, $\alpha_h = \text{diag}\{0.01,0.01,0.01\}$, $\alpha_{en} = \text{diag}\{0.07,0.1,0.09\}$, $\alpha_t = \text{diag}\{0,0,0.02\}$, $t_t = 0.2$s, $Kr = \text{diag}\{31.4,31.4,31.4\}$, Γ = {10e-8, 10e-9, 10e-9; 10e-8, 10e-9, 10e-9}, $K_h = \text{diag}\{1,1,3\}$, $K_s = \text{diag}\{0.6,0.4,0.4\}$, $\Lambda_{sv} = \text{diag}\{3,3,3\}$, $\Lambda_{sp} = \text{diag}\{5,5,5\}$ and sample time = 0.002s. Practically, a simple way to ensure $\hat{B}_d$ to be positive definite is to set a minimal value that is obtained empirically [10]. Another practical note is to use low-past-filter and saturation [6] for F_h. Additionally, the initial values of the dynamic model $\hat{a}$ is obtained by the properties from the datasheets.

B. Experiment 1: Transition in the Position Maintaining Axis

For experiment 1, a human operator guides the robot to a target position in AgM and switches into AutM. The goal is to test the transition in the position maintaining axis using the proposed control scheme. For simplicity of illustration, we conduct only 1 DOF (X axis). Additionally, we compare our method with traditional controller where force control is employed in AgM and a position controller (20Hz bandwidth) is used in AutM. For a fair comparison, we tune the parameters of the force controller in AgM and position controller in AutM in the traditional method to ensure that the performance is stable in each mode independently. In addition, the transition time is the same, i.e., $t_t = 0.2$. During the transition, the force control command reduces to 0 and position control command increases to the target position.

The results are shown in Fig. 5 (A). Since there is no environment in the position maintaining axis, the transition happens between pHRI and pREI. Due to the change of the control scheme in the traditional controller, the maximum position overshoot is 5.82 mm with the oscillation. This amount of overshoot is significant for the application that requires precise alignment such as the assembly of the phone. Contrarily, the position overshoot in the proposed control scheme is close to 0 mm which results in smooth transition. One thing to take note is that the motion in pHRI is completed by human. Hence, there is an inevitably slight difference for the final target position between two controllers.

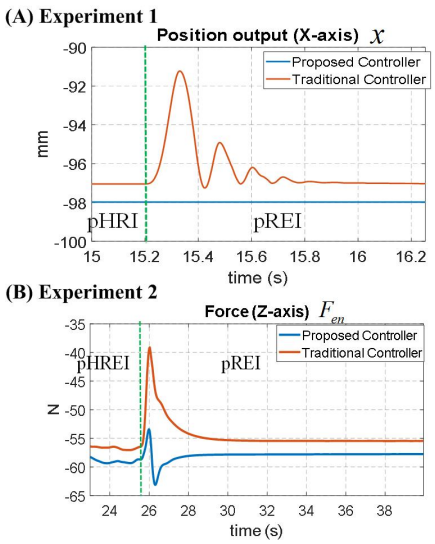

Fig. 5. Results of experiment 1 and 2. (A) Exp 1: Transition in the position maintaining axis. (B) Exp 2: Transition in the contacting axis.

TABLE I

Experimental Results: Max Overshoot During the Transition

Exp	Proposed	Traditional
Exp1	0 mm	5.82 mm with oscillation
Exp2	5.20 N	17.21 N
Exp3	0.1 mm in the position maintaining axis 3.75 N in the contacting axis	N/A

C. Experiment 2: Transition in the Contacting Axis

In experiment 2, the transition in the contacting axis is validated. The human operator guides the robot in AgM to contact the wooden platform using a sufficient force, then switches the controller scheme to AutM after the interaction is stabilized. We compare the proposed method with traditional VAC used for pHREI [10]. The conditions for the traditional VAC are: (i) the proposed transition term in variable damping (10) is not considered; (ii) the transition time is the same with the proposed one; and (iii) VAC is

used for both AgM and AutM but the desired force is from human in AgM while it is a constant force in AutM (same with proposed method). In addition, for a fair comparison on both sets of controllers, the human operator practices a few times to "feel" the maintaining forces. During the experiment, the human operator looks at the monitor that displays the online human force F_h and tries to execute the same maintaining force (although there is still inevitably a slight difference between two sets).

The results are shown in Fig. 5 (B). The human maintaining forces for both controllers are roughly 18∼19 N and environmental forces are about -55 N to -58 N in pHREI. However, due to the lack of transition term in the update law for the traditional VAC, the environmental force drops significantly during the transition. The maximal drop is 17.21 N which is about the human force in pHREI. On the other hand, with the proposed method, the contacting force drops 5.2 N with 2.05 seconds oscillation (1.5 N steady-state error). This results in a smoother transition.

D. Experiment 3: Application

The last evaluation is the application using the robot with the proposed controller. In experiment 3, a mock-up of a simplified phone assembly using adhesive strips is tested. As shown in Fig. 4 (C), the mock-up validation is a 3D printed phone and a 3D printed screen with adhesive strips. At the beginning of the experiment, the screen is placed on the top of the phone. The phone and the screen are aligned with adhesive strips in between, with the phone placed on the wooden platform of the environment. The operator moves the robot to exert sufficient force on the phone. After the interaction is stable, the controller scheme is switched into AutM and the robot autonomously presses the phone for 30 seconds in absence with human. In the end, the human switches the controller to AgM and moves the robot away.

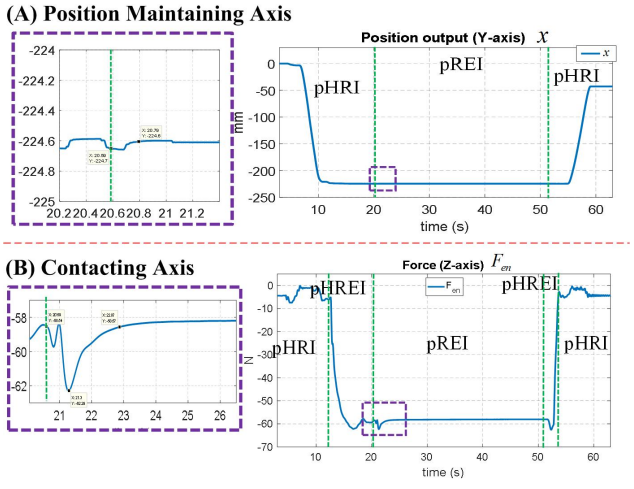

Fig. 6. Experiment 3: (A) Transition in the position maintaining axis and (B) transition in the contacting axis.

The transitions are shown in Fig. 6. In the position maintaining axis, it can be observed that the transitions between each interaction are smooth. In the contacting axis, due to the sudden drop of the net force after human releases the robot, the environmental force slightly fluctuates during the transition from pHREI to pREI. However, when using the proposed controller, the environmental force is stabilized within 2.28 seconds with a small 3.75 N overshoot and 2.63 % (1.5N / 57.07N) steady-state error. The smooth transition and the stable interaction for this application demonstrate the capability of the proposed controller. This also demonstrates our contribution.

E. Potential Applications and Limitations

While the significance might still have room for improvement, the proposed control scheme benefits the potential applications as it can utilize human knowledge in semi-autonomous tasks, and the advantage of a robot such as high power or accuracy in fully autonomous tasks. Other than medical robots [11] and the phone assembly, it can also be applied as a rehabilitative robot [21], [31] where the augmentation mode provides the strength to the patient and the autonomous mode can serve as a resistance that trains the patient's muscles. Another example is a grinding robot [33] in a clutter environment. The user can guide the robot to the desired position in a dynamic environment, which is challenging for a camera to identify, followed by the autonomous mode where the robot can automatically grind a certain area. Another promising application is Series Elastic Actuators (SEA) [31], [34]. The human operator guides the robot to the desired position with his/her desired impedance in the augmentation mode, a control scheme with the variable stiffness actuators adapts the impedance to finish a task in the autonomous mode.

Although the proposed control scheme shows a promising result, like all other conventional/existing methods, there are still some limitations to be rectified to further expand the potential practical applications. Firstly, to fulfill the stability during the transition, the switch of the control scheme must happen when the robot motion is stationary and desired motion is zero, i.e. $\dot{x}_m = 0$ and $\dot{x}_d = 0$. It would be interesting to explore the control design that allows the transition during the movement. This leads to broader application such as medical robot [10] where the surgeon can target a moving stone and followed by tracking of the robot after the switch of the control modes without stopping patient's breath. Secondly, we only investigate the application without any payload so the force estimation employed in this paper is based on a constant dynamic [22]. In addition, the convergence of the force estimation is under assumption of slow-time varying force change [29], [30]. This limits the application where the weights the load must be known before the operation and rapid force impact is not allowed. Investigating a more advanced force estimator, such as sliding mode momentum observers [32], to overcome the limits is a promising topic for future work.

V. CONCLUSION

In this paper, we have addressed the cobot issue of unstable transition from an augmentation mode to an autonomous

mode in physical human-robot-environment interaction. A control scheme that unifies impedance/admittance in the outer loop and unifies adaptive position/velocity control in the inner loop is proposed. A transition factor is proposed to switch between two modes. Additionally, human and environmental forces are measured separately to update the admittance or impedance with the corresponding interaction, which leads to the smooth transition. Experiments are conducted to demonstrate the capability where the human can guide the robot in pHRI, stably contact an environment in pHREI, smoothly transits the interaction to pREI and the robot can autonomously maintain the same position while keeping the contacting force with the environment. We have also verified the proposed idea in the application of the assembly of the phone during NPI. The control scheme is switched within 0.2 second and this smooth transition is achieved with maximum overshoots of 0.1mm in the position maintaining axis and 3.75N in the contacting axis.

To the best of authors' knowledge, this work is the first to explore the controller transition for a cobot during pHREI from augmentation to autonomous mode, which serves as the main contribution. This proposed method is particular interesting since human can choose semi-autonomous/augmentation or fully autonomous function depending on the task. The future work is to open up new possibilities in the ways the intelligence of cobot is being enhanced using the concept of the transition between each interaction.

REFERENCES

[1] C. T. Landi, F. Ferraguti, L. Sabattini, C. Secchi, and C. Fantuzzi, "Admittance control parameter adaptation for physical human-robot interaction," *IEEE Int. Conf. Robot. Autom.*, pp. 2911-2916, 2017.

[2] F. Ficuciello, L. Villani and B. Siciliano, "Variable impedance control of redundant manipulators for intuitive human–robot physical interaction," *IEEE Trans. Robot.*, vol. 31, no. 4, pp. 850-863, Aug. 2015.

[3] J. Krüger, and D. Surdilovic, "Robust control of force-coupled human-robot-interaction in assembly processes", *CIRP Annals - Manufacturing Technology*, vol. 57, no. 1, pp. 41-44, 2008.

[4] R. Taylor *et al.*, "Steady-hand robotic system for microsurgical augmentation," *Int. J. Robot. Res.*, vol. 18 no. 12, pp. 1201-1210, 1999.

[5] F. Ferraguti, C. T. Landi, L. Sabattini, C. Fantuzzi, and C. Secchi, "A variable admittance control strategy for stable physical human – robot interaction," *Int. J. Rob. Res.*, 2019.

[6] A. Lecours, B. Mayer-St-Onge and C. Gosselin, "Variable admittance control of a four-degree-of-freedom intelligent assist device," in *Proc. IEEE Int. Conf. Robot. Autom.*, pp. 3903-3908, 2012.

[7] H.-Y. Li, N. Theshani, A.X. Sebaratnam, and U-Xuan Tan. "Human-micromanipulator cooperation using a variable admittance controller." *Sci. China Inf. Sci.*, vol. 62, no. 5, 2019.

[8] P. D. Labrecque, T. Laliberté, S. Foucault, M. E. Abdallah and C. Gosselin, "uMan: A low-impedance manipulator for human–robot cooperation based on underactuated redundancy," *IEEE/ASME Trans. Mechatronics*, vol. 22, no. 3, pp. 1401-1411, June 2017.

[9] P. D. Labrecque and C. Gosselin, "Variable admittance for pHRI : From intuitive unilateral interaction to optimal bilateral force amplification," *Robot. Comput. Integr. Manuf.*, vol. 52, no. 2018, pp. 1–8, 2018.

[10] H. Li *et al.*, "Stable and compliant motion of physical human–robot interaction coupled With a moving environment using variable admittance and adaptive control," *IEEE Robotics and Automation Letters*, vol. 3, no. 3, pp. 2493-2500, July 2018.

[11] H.-Y. Li *et al.*, "Towards to a robotic assisted system for percutaneous nephrolithotomy," in *Proc. IEEE/RSJ Int. Conf. Intell. Robots Syst.*, pp. 791-797, 2018.

[12] N. Hogan, "Impedance control: An approach to manipulation: Part I - Theory," *J. Dyn. Sys., Meas., Control*, vol. 107, pp. 1–7, 1985.

[13] Y. Li and S. S. Ge, "Impedance learning for robots interacting with unknown environments," *IEEE Trans. on Control Systems Technology*, vol. 22, no. 4, pp. 1422-1432, July 2014.

[14] Seul Jung, T. C. Hsia and R. G. Bonitz, "Force tracking impedance control of robot manipulators under unknown environment," *IEEE Trans. on Control Systems Technology*, vol. 12, no. 3, pp. 474-483, May 2004.

[15] T.-J. Tarn, *et al.*. "Force regulation and contact transition control." IEEE Control Systems Magazine vol. 16, no. 1, pp. 32-40, 1996.

[16] C. Ott, R. Mukherjee and Y. Nakamura, "Unified impedance and admittance Control," in *Proc. IEEE Int. Conf. Robot. Autom.*, pp. 554-561, 2010.

[17] J. Wu, F. Ni, Y. Zhang, S. Fan, Q. Zhang, J. Lu, and H. Liu, "Smooth transition adaptive hybrid impedance control for connector assembly", *Industrial Robot: An International Journal*, 2018.

[18] M. H. Raibert, and J. J. Craig, "Hybrid position/force control of manipulators", *J. Dyn. Syst. Meas. Control*, vol. 103, no. 2, pp. 126-133, 1981.

[19] H.-Y. Li *et al.*, "A control scheme for physical human-robot interaction coupled with an environment with unknown stiffness," *J. Intell. Robot. Syst.*, 2020.

[20] X. Li, G. Chi, S. Vidas and C. C. Cheah, "Human-guided robotic comanipulation: Two illustrative scenarios," *IEEE Trans. on Control Systems Technology*, vol. 24, no. 5, pp. 1751-1763, Sept. 2016.

[21] J. Zhang and C. C. Cheah, "Passivity and stability of human – robot interaction control for upper-limb rehabilitation robots," *IEEE Trans. Robot.*, vol. 31, no. 2, pp. 233–245, 2015.

[22] A. D. Luca, A. Albu-Schaffer, S. Haddadin and G. Hirzinger, "Collision detection and safe reaction with the DLR-III lightweight manipulator arm," in *Proc. IEEE/RSJ Int. Conf. Intell. Robots Syst.*, pp. 1623-1630, 2006.

[23] Chien-Chern Cheah and Danwei Wang, "Learning impedance control for robotic manipulators," *IEEE Trans. Robot. Autom.*, vol. 14, no. 3, pp. 452-465, June 1998.

[24] C. I. Byrnes, A. Isidori and J. C. Willems, "Passivity, feedback equivalence, and the global stabilization of minimum phase nonlinear systems," *IEEE Trans. on Automatic Control*, vol. 36, no. 11, pp. 1228-1240, Nov. 1991.

[25] A. Albu-Schaffer, C. Ott, and G. Hirzinger, "A unified passivity-based control framework for position torque and impedance control of flexible joint robots", *Int. J. Robot. Res.*, vol. 26, no. 1, pp. 23-39, 2007.

[26] S. Lee, M. Kim and J. Song, "Sensorless collision detection for safe human-robot collaboration," in *Proc. IEEE/RSJ Int. Conf. Intell. Robots Syst.*, pp. 2392-2397, 2015.

[27] Y. Pan, C. Yang, L. Pan, and H. Yu, "Integral sliding mode control: Performance, modification and improvement," *IEEE Trans. Ind. Informatics*, vol. 14, no. 7, pp. 3087–3096, 2018.

[28] J.J. Slotine and W. Li, "Applied nonlinear control," Englewood Cliffs, NJ, *USA: Prentice-Hall*, 1991.

[29] A. Nikoobin, and R. Haghighi, "Lyapunov-based nonlinear disturbance observer for serial n-link robot manipulators," *J. Intell. Robot. Syst.*, vol. 55, pp. 135-153, 2009.

[30] H. Sadeghian, L. Villani, M. Keshmiri, and B. Siciliano, "Task-space control of robot manipulators with null-space compliance," *IEEE Trans. Robot.*, vol. 30, no. 2, pp.493-506, 2013.

[31] X. Li, Y.-H. Liu, and H. Yu, "Iterative learning impedance control for rehabilitation robots driven by series elastic actuators," *Automatica*, vol. 90, pp.1-7, 2018.

[32] G. Garofalo, N. Mansfeld, J. Jankowski and C. Ott, "Sliding mode momentum observers for estimation of external torques and joint acceleration," in *Proc. IEEE Int. Conf. Robot. Autom.*, pp. 6117-6123, 2019.

[33] M. Jinno *et al.*, "Development of a force controlled robot for grinding, chamfering and polishing," in *Proc. IEEE Int. Conf. Robot. Autom.*, vol.2, pp. 1455-1460, 1995.

[34] D. P. Losey, A. Erwin, C. G. McDonald, F. Sergi and M. K. O'Malley, "A time-domain approach to control of series elastic actuators: Adaptive torque and passivity-based impedance control," *IEEE/ASME Trans. Mechatronics*, vol. 21, no. 4, pp. 2085-2096, Aug. 2016.

[35] A. Karami, H. Sadeghian, M. Keshmiri, and G. Oriolo, "Hierarchical tracking task control in redundant manipulators with compliance control in the null-space," *Mechatronics*, vol. 55, pp. 171-179, 2018.